Mathematical Biosciences and Engineering

MBE, 19(2): 1843–1860.
DOI: 10.3934/mbe.2022086
Received: 03 September 2021
Accepted: 24 November 2021
Published: 20 December 2021

http://www.aimspress.com/journal/MBE

Research article

Identification of novel immunomodulators in lung squamous cell carcinoma based on transcriptomic data

Xin Lin[1,†], Xingyuan Li[2,†], Binqiang Ma[1,†] and Lihua Hang[1,*]

[1] Department of Anesthesiology, Medical College of Soochow University, Affiliated Kunshan Hospital of Jiangsu University, Kunshan 215399, China
[2] Department of Anesthesiology, Kunshan Fourth People's Hospital, Kunshan 215399, China

* **Correspondence:** Email: mumu_7239@163.com; Tel: +8618013288480; Fax: +051257519685.

† These authors contributed equally to this work.

Abstract: Cells in the tumor microenvironment are well known for their role in cancer development and prognosis. The processes of genetic changes and possible remodeling in the tumor microenvironment of lung squamous cell carcinoma, on the other hand, are mainly unclear. In this investigation, 1164 immunological differentially expressed genes (DEGs) were shown to have predictive significance. A prognostic model with high prediction accuracy was constructed using these genes and survival data. There were 1020 upregulated genes and 144 downregulated genes found, with 57 genes found to be important in the development of LUSC. We used least absolute shrinkage and selection operator (LASSO) regression analysis to determine the risk profiles of 9 genes based on the expression values of 57 prognosis-related genes. The AUCs of the developed prognostic model for predicting patient survival at 1, 3, and 5 years were 0.66, 0.61, and 0.63, respectively, based on the training data. For immune-correlation analysis in this survival model, we chose IGLC7, which was seen to predict patient survival with high accuracy. The effects on immune cells and synergistic effects with other immunomodulators were then investigated. We discovered that IGLC7 is involved in immune response and inflammatory activity using gene ontology analysis and genomic sequence variance analysis (GSVA), with a potential effect, especially on B cells and T cells. In conclusion, IGLC7 expression levels are related to the malignancy of LUSC based on the constructed prognostic model and can thus be a therapeutic target for patients with LUSC. Furthermore, IGLC7 may work in concert with other immune checkpoint members to regulate the immune microenvironment of LUSC. These discoveries might lead to a fresh understanding of the complicated interactions between cancer cells and the tumor microenvironment, particularly the population of

immune cells, and a novel approach to future immunotherapeutic treatments for patients with LUSC.

Keywords: IGLC7; immunotherapy; lung squamous cell carcinoma

1. Introduction

Lung cancer is one of the most lethal cancers in the world, and it is classified into two kinds: small cell lung cancer (SCLC) and non-small cell lung cancer (NSCLC). NSCLC accounts for approximately 85% of lung cancer cases and is mainly divided into two categories based on etiology and histological pattern: lung adenocarcinoma (LUAD) and lung squamous cell carcinoma (LUSC) [1,2]. Lung cancer is treated with various treatments, including surgical resection, chemotherapy, radiotherapy, targeted therapy, and immunotherapy [3]. Surgical resection is used to treat patients with early-stage NSCLC. Because the tumor cannot be physically removed, the best therapeutic option for patients in advanced stages of NSCLC is targeted therapy or immunotherapy coupled with chemotherapy [4].

Since inhibitors of epidermal growth factor receptor (EGFR), anaplastic lymphoma kinase (ALK), and vascular endothelial growth factor (VEGF) became available in the early twenty-first century, patients with advanced LUAD had a better prognosis [5]. Patients with LUSC, on the other hand, did not have similar increases in survival; this might be because most lung cancer therapy breakthroughs in the last decade have improved the prognosis for adenocarcinoma, but not for LUSC [6]. The current slate of options for squamous lung cancer therapy is limited.

Understanding and researching possible molecular targets for LUSC might identify new methods for treating this kind of lung cancer. After immune checkpoint therapy (ICB), a type of therapy that utilizes checkpoint inhibitors to allow the immune system to recognize and attack tumor cells, some LUSC patients continue to develop further, and treatment results are poor [7]. Some cytokines, such as IL-6, enable tumor cells to evade immune monitoring by promoting the stemness of LUSC cells in the tumor microenvironment [8]. Evasion of immune surveillance and chronic inflammation are hallmarks of tumor growth in all tumor tissues, including LUSC [9]. In this study, we investigated differentially-expressed genes (DEGs) in LUSC. After analyzing these genes and their pathways, a prognosis-related core gene set was constructed, and survival models were built using multifactorial Cox regression. This resulted in a better understanding of occurrence and development processes of LUSC and its prognosis. We selected IGLC7, the survival model's key gene, for further investigation.

To date, the mechanisms underlying the oncogenic role of IGLC7 in lung cancer remain mostly unknown. In our study, we found that IGLC7 is involved in the control of several immune-related pathways, suggesting its possible role in the immune microenvironment. However, to date, no mechanism has been reported regarding the immunological role of IGLC7 in cancer. Here, we explored the association of IGLC7 with immune cells and analyzed how it is involved in immune regulatory mechanisms. Our findings demonstrate a role for IGLC7 in tumor immunity, suggesting that IGLC7 may be a potential immunotherapeutic target for LUSC.

2. Materials and methods

2.1. Data collection

The Cancer Genome Atlas (TCGA) (https://www.cancer.gov/about-nci/organization/ccg/research/structural-genomics/tcga) and the University of California, SantaCruz (UCSC) Xena (https://xenabrowser.net/datapages/) databases were used to obtain gene expression profiles and clinical information for LUSC patients, including gender, age, histopathological type, and survival data. We used the ESTIMATE algorithm to calculate the immune/stromal scores and the ESTIMATE scores for LUSC patients (https://bioinformatics.mdanderson.org/estimate/rpackage.html). The immune cell marker gene set used for Gene Set Variation Analysis (GSVA) was obtained from Gabriela et al. [10].

2.2. Identification of immune DEGs

DEG calculation was conducted using R software (version 3.6.0; https://www.r-project.org/) and the limma package [11]. The cutoffs for screening of immune DEGs were absolute fold change ≥ 1.5 and adjusted p-value < 0.05.

2.3. Bioinformatics analysis

The Cluster Profiler R package was used for gene ontology (GO) analysis of genes associated with the immune response. KEGG (Kyoto Encyclopedia of Genes and Genomes) analysis was also performed to identify enriched pathways. The Microenvironment Cell Populations-counter (MCP-counter) method was used to calculate the absolute abundance of immunological cell populations. Scores of gene sets associated with immunological functions and inflammatory activities were calculated using GSVA.

2.4. Statistical analysis

The R programming language was used for all statistical testing. The correlations between continuous variables were estimated using the Wilcoxon and Kruskal-Wallis tests. Cox proportional hazards model analysis was used to assess IGLC7's prognostic value. The R packages ggplot2, pheatmap, survival ROC, circlize, and corrplot were used to further statistical computations and graphical work, and a statistically significant difference was defined as p-value < 0.05.

2.5. Survival model construction

We use the R package glmnet to perform lasso cox regression for the analysis. First, we analyze the trajectory of each independent variable, and in the training set we perform 1000 lasso regression analyses, followed by model construction using 10-fold cross-validation, and then aggregate the results of each downscaling, counting the number of occurrences of each probe in 100 times, where the combination of the maximum frequency of occurrence can be observed.

3. Results

3.1. Correlation of immune, stromal, and ESTIMATE scores with clinical subgroup information in lung squamous cell carcinoma

Figure 1. Immune, stromal, and ESTIMATE Scores are associated with LUSC.

The TCGA and UCSC Xena (https://xenabrowser.net/datapages/) databases were used to obtain gene

expression profiles, demographics, and clinical characteristics of 496 LUCS samples. After analysis, we found that the 496 LUSC cases had immunological scores distributed between -1646.821 and 3063.732, stromal scores between -2286.256 and 1799.134, and ESTIMATE scores between -3414.484 and 4445.312. Separating results based on tumor staging, the three scores for stages I-III became concentrated relative to stage IV, although it was not statistically significant (n.s., not significant; $*p < 0.05$, $***p < 0.01$). For the T, N, and M stages, no significant differences were seen across stages. However, immune scores and stromal scores significantly differed between the sexes, suggesting the potential significance of immune, stromal, and ESTIMATE scores in differentiating clinical features (Figure 1).

In addition, we assessed the potential association between overall survival and immune score. Using the immune score obtained from the ESTIMATE algorithm, we divided the 496 LUSC cases with both immune score and survival data into two subgroups: high a (score ≥ 0) and low (score < 0). Kaplan-Meier curves showed that between these two groups, the prognosis of the high-scoring group was worse than that of the low-scoring group, and the difference was significant ($p = 0.039$); This result suggests that the immune score enables a certain degree of sample classification into high- and low-risk groups (Figure 2).

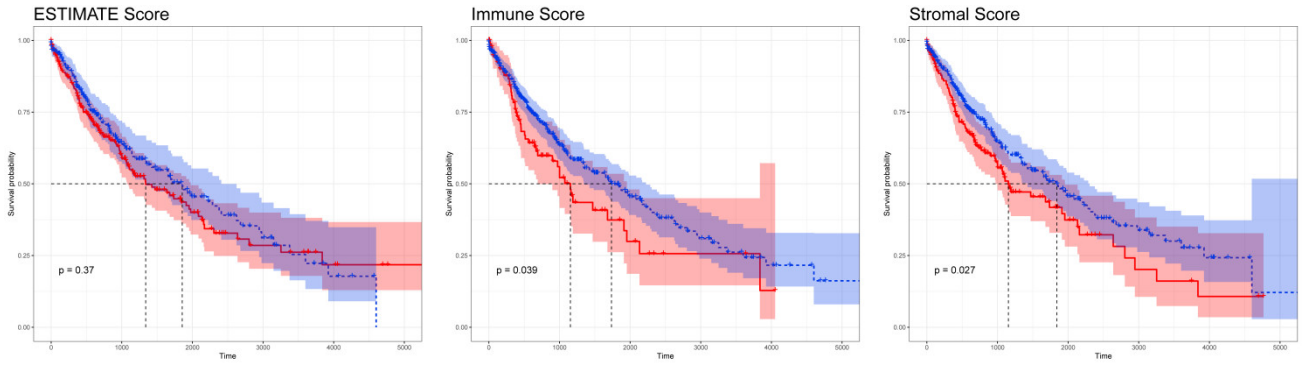

Figure 2. KM survival curves plotted by grouping immune, stromal and ESTIMATE scores into high and low scoring groups.

3.2. Differential expression and functional enrichment of immune-microenvironment-related gene features in lung squamous cell carcinoma

To assess the relationship between whole gene expression profiles and immune scores, we compared high immune score subgroups with low immune score subgroups and screened for upregulated and downregulated differential genes. We defined the genes identified here as immune DEGs. The hierarchical clustering heat map shows the expression profiles of the top 15 upregulated and downregulated genes in the high- and low-immune score groups (Figure 3A). Among all DEGs (Figure 3A), 1020 genes showed significant upregulation, while 144 genes showed significant downregulation. We further performed follow-up analyses to elucidate the potential functions of immune-microenvironment-related DEGs (immune DEGs).

The relevance of certain functions was alluded to by the enrichment factor of GO and KEGG pathway analyses. Immune DEGs were particularly enriched in the following categories in the GO analysis: lymphocyte-mediated immunity, immune response-activating cell surface receptor signaling pathway), adaptive immune response based on somatic recombination of immune receptors built from

immunoglobulin superfamily domains, immunoglobulin complex, external side of plasma membrane, and antigen binding. Immune DEGs were significantly enriched in the hematopoietic cell lineage, cytokine-cytokine receptor interaction, Staphylococcus aureus infection, and cell adhesion molecules pathways in the KEGG pathway study (Figure 3B,C). GSEA analysis mainly showed significant differences in gene expression in cellular calcium ion homeostasis, receptor-ligand activity, regulation of GTPase activity, calcium signaling pathway, and cytokine-cytokine receptor interaction (Figure 3D,E).

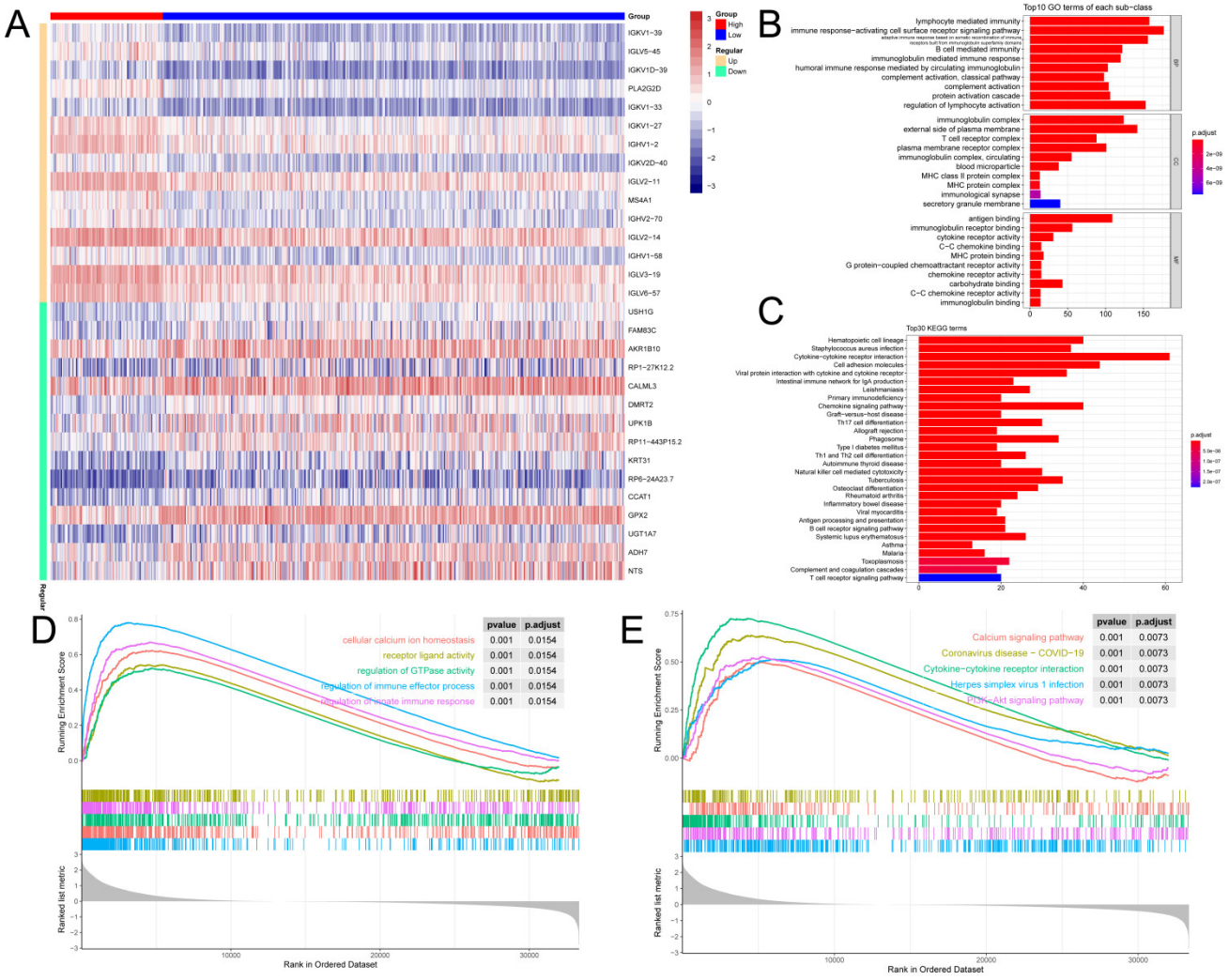

Figure 3. DEGs, GO, KEGG, and GSEA results for immune scores of patients with LUSC. (A) Hierarchical cluster profiles of immune DEGs in LUSC. (B) GO analysis of immune DEGs. The y axis refers to GO categories. (C) The KEGG pathway analysis of immune DEGs. The y axis refers to pathway terms. (D, E) The major pathways in GSEA enrichment analyses.

3.3. Identification and analysis of immune DEGs with prognostic value

We used a cross-set analysis of immune DEGs and survival significance genes to find more immune cell-related genes with prognostic value. Of the 1164 previously screened immune DEGs and the 3990 survival significance genes culled from the bulk survival data analysis (Figure 4A), 57

immune DEGs were found to be present in both and thus potentially be of prognostic value in patients with LUSC (Table 1). To further understand the mechanism of action of this gene set, we focused on the potential functions of the 57 intersection genes. Pathway analysis showed that these were mainly enriched in hematopoietic cell lineage, cytokine-cytokine receptor interaction and Staphylococcus aureus infection. In the GO report, the genes were mainly enriched in the acute inflammatory response, platelet degranulation, and positive regulation of protein secretion (Figure 4B,D, Table 2).

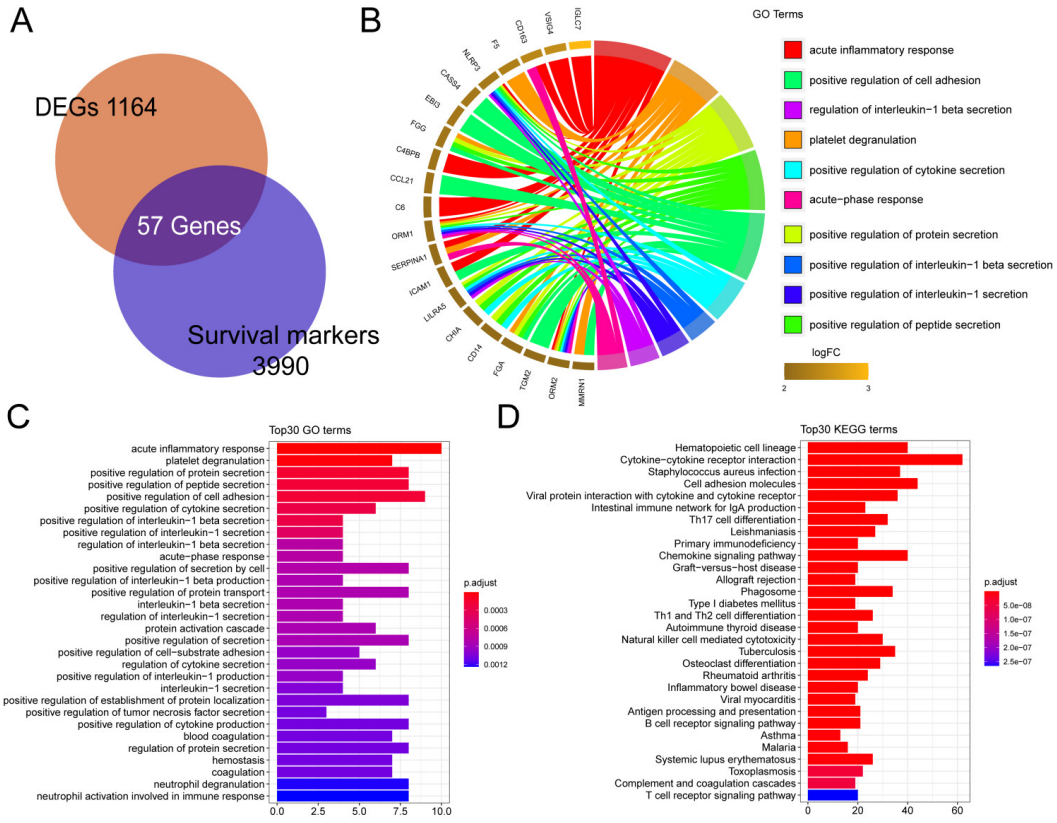

Figure 4. GO and KEGG analyses for immune DEGs of prognostic value. (A) Venn diagram showing the number of intersections of genes of survival significance in all immune DEGs and LUSC. (B) Circle plot depicting the important signal pathways associated with those genes. (C) GO analysis for immune DEGs of prognostic value. The y axis refers to GO categories. (D) KEGG pathway analysis. The y axis refers to pathway terms.

Table 1. A gene set that affects both patient survival and immune status.

SYMBOL	logFC	AveExpr	t	P.Value	adj.P.Val	B
IGLC7	2.548505035	7.092407712	8.366919343	6.08E-16	2.26E-14	25.42401274
RP6-24A23.7	-2.246899246	4.239234465	-6.213775629	1.10E-09	2.01E-08	11.33596777
ADH1B	2.072175752	7.452303717	6.469897792	2.36E-10	4.78E-09	12.83192397
IRS4	-2.018163853	3.550377757	-5.720254073	1.84E-08	2.77E-07	8.600255952
VSIG4	1.99112673	9.884367377	11.44186452	4.67E-27	4.43E-25	50.64025187
GSTA9P	-1.988172032	4.933903412	-4.938665953	1.08E-06	1.16E-05	4.67770443
SLCO2B1	1.978099287	10.93047821	12.78118783	1.59E-32	2.36E-30	63.07951296

Continued on next page

SYMBOL	logFC	AveExpr	t	P.Value	adj.P.Val	B
CD163	1.917159005	11.08072239	11.28812503	1.88E-26	1.71E-24	49.26180047
LINC01133	-1.900159056	8.048896879	-5.839933851	9.47E-09	1.51E-07	9.245639947
MRC1	1.859425416	9.964262079	9.996326226	1.49E-21	9.43E-20	38.13590862
ACSL5	1.85924314	9.820614368	11.8059225	1.64E-28	1.73E-26	53.94693942
F5	1.817700041	7.361125217	9.957749159	2.06E-21	1.29E-19	37.8170195
MAP1LC3C	1.815530211	3.462553234	9.869245583	4.31E-21	2.62E-19	37.08852473
CLIC5	1.784177736	7.942989577	9.259881222	6.22E-19	3.11E-17	32.1933696
NLRP3	1.723862492	6.984305517	12.76902715	1.79E-32	2.62E-30	62.96333467
RP6-24A23.3	-1.717984124	3.367299692	-5.939441084	5.39E-09	8.91E-08	9.791088366
GPRIN3	1.715719809	9.077932075	14.55330225	3.39E-40	1.45E-37	80.54743529
CASS4	1.712066279	7.317498174	12.49919541	2.39E-31	3.25E-29	60.39990935
EBI3	1.707628673	6.681178313	12.83644646	9.31E-33	1.42E-30	63.6081262
FGG	1.672298396	7.13182914	3.909269008	0.000105481	0.000700173	0.316122109
CYP1B1	1.671985675	10.7972337	9.963955678	1.96E-21	1.23E-19	37.86826917
NFATC2	1.671214524	8.938921136	12.7998645	1.33E-32	2.00E-30	63.25804987
ALOX5	1.665187367	10.01843216	12.12097666	8.64E-30	9.99E-28	56.85491279
ADAMTS16	1.658381412	6.72653592	7.521682756	2.57E-13	7.37E-12	19.49647401
C4BPB	1.658183898	3.724989671	7.214420841	2.05E-12	5.32E-11	17.46518648
FOLR2	1.64762722	8.83428587	10.07853333	7.46E-22	4.83E-20	38.81817144
HNF1B	1.642458056	5.013620202	6.145173695	1.64E-09	2.92E-08	10.94402813
CCL21	1.636421059	10.13311209	8.032703951	7.03E-15	2.37E-13	23.02213038
TRAV39	1.626839219	2.311039799	11.70632233	4.12E-28	4.19E-26	53.03646265
CD300LG	1.617895237	2.44910609	7.987238929	9.75E-15	3.24E-13	22.70117307
MYO1G	1.615070833	9.592895949	12.98669569	2.16E-33	3.52E-31	65.05112688
EMR4P	1.609011782	4.515705823	10.38105571	5.66E-23	3.96E-21	41.36019382
VSTM2L	1.60480087	7.508223212	6.914963584	1.45E-11	3.43E-10	15.55164859
CCDC141	1.604041691	4.624710837	8.828632019	1.84E-17	7.92E-16	28.8619323
RP11-24F11.2	1.594541963	4.155966853	12.28521815	1.83E-30	2.27E-28	58.38725887
SPNS3	1.594132963	4.531398814	12.19595584	4.26E-30	5.07E-28	57.55308966
C6	1.592539459	3.965568725	5.780446584	1.32E-08	2.05E-07	8.923391746
RP11-327F22.2	1.579229878	3.63713198	13.46760369	1.92E-35	4.06E-33	69.72372586
ORM1	1.574045514	4.85723254	5.498021786	6.16E-08	8.51E-07	7.432982769
SIGLEC12	1.573947153	5.743410454	7.182648624	2.53E-12	6.52E-11	17.25903455
SERPINA1	1.572377945	12.71759883	7.638476848	1.15E-13	3.40E-12	20.28624902
RNASE2	1.56823968	5.143037891	10.81623415	1.28E-24	1.02E-22	45.10036314
ICAM1	1.563326022	12.08334689	10.40717018	4.52E-23	3.19E-21	41.58189671
LILRA5	1.554817662	6.96200275	10.83511174	1.08E-24	8.67E-23	45.26476666
GDF10	1.551427458	4.439058564	6.70029826	5.67E-11	1.25E-09	14.22105768
PDK4	1.550621108	8.522807089	7.775475879	4.40E-14	1.36E-12	21.22484133
CHIA	1.550460435	3.328010566	5.484928478	6.61E-08	9.07E-07	7.365482938
CD14	1.550043738	11.68969949	12.75548812	2.04E-32	2.96E-30	62.83405333
FGA	1.549965786	5.297010469	4.185131318	3.37E-05	0.000254721	1.392620042

Continued on next page

SYMBOL	logFC	AveExpr	t	P.Value	adj.P.Val	B
TGM2	1.542232915	13.06535281	10.08347407	7.15E-22	4.64E-20	38.85929337
TM6SF1	1.53437298	6.596339654	12.26404081	2.24E-30	2.75E-28	58.18906126
CCDC69	1.533136364	10.11306613	13.08957788	7.92E-34	1.37E-31	66.04393452
ORM2	1.529208475	3.86207309	6.185867726	1.30E-09	2.34E-08	11.17607384
TFPI2	1.518397722	7.668569517	5.763912449	1.45E-08	2.22E-07	8.834335969
LILRB3	1.51130062	7.146562684	13.04647337	1.21E-33	2.04E-31	65.62751636
FCGR2A	1.510736169	10.74624564	11.27934	2.04E-26	1.84E-24	49.18336229
MMRN1	1.503686425	7.18831982	7.930081867	1.47E-14	4.79E-13	22.29966924

Table 2. Survival immunity-associated gene set GO functional enrichment pathway.

ID	Description
GO:0002449	lymphocyte mediated immunity
GO:0002429	immune response-activating cell surface receptor signaling pathway
GO:0002460	adaptive immune response based on somatic recombination of immune receptors built from immunoglobulin superfamily domains
GO:0019724	B cell mediated immunity
GO:0016064	immunoglobulin mediated immune response
GO:0002455	humoral immune response mediated by circulating immunoglobulin
GO:0006958	complement activation, classical pathway
GO:0006956	complement activation
GO:0072376	protein activation cascade
GO:0051249	regulation of lymphocyte activation
GO:0006959	humoral immune response
GO:0006909	phagocytosis
GO:0050867	positive regulation of cell activation
GO:0002696	positive regulation of leukocyte activation
GO:0051251	positive regulation of lymphocyte activation
GO:0050851	antigen receptor-mediated signaling pathway
GO:0002377	immunoglobulin production
GO:0002697	regulation of immune effector process
GO:0050853	B cell receptor signaling pathway
GO:0002920	regulation of humoral immune response
GO:0002440	production of molecular mediator of immune response
GO:0030449	regulation of complement activation
GO:2000257	regulation of protein activation cascade
GO:0050900	leukocyte migration
GO:0042113	B cell activation
GO:0050864	regulation of B cell activation
GO:0002673	regulation of acute inflammatory response
GO:0006911	phagocytosis, engulfment
GO:0002526	acute inflammatory response
GO:0099024	plasma membrane invagination

3.4. Prognostic implication of IGLC7-associated immunomodulators in lung cancer

We generated a 9-gene LUSC prognostic profile. We then split the samples 1:1 to form a training set and a test set, and tested this risk model in the training set versus the overall data set (Figure 5A). The model was evaluated using Kaplan-Meier survival curves with cox p = 0.0017 in the training set and cox p < 0.0001 in the overall dataset (Figure 5B). According to the ROC curves, the ROC values were greater than 0.6 in both the training set as well as the overall dataset, indicating good predictive performance (Figure 5C).

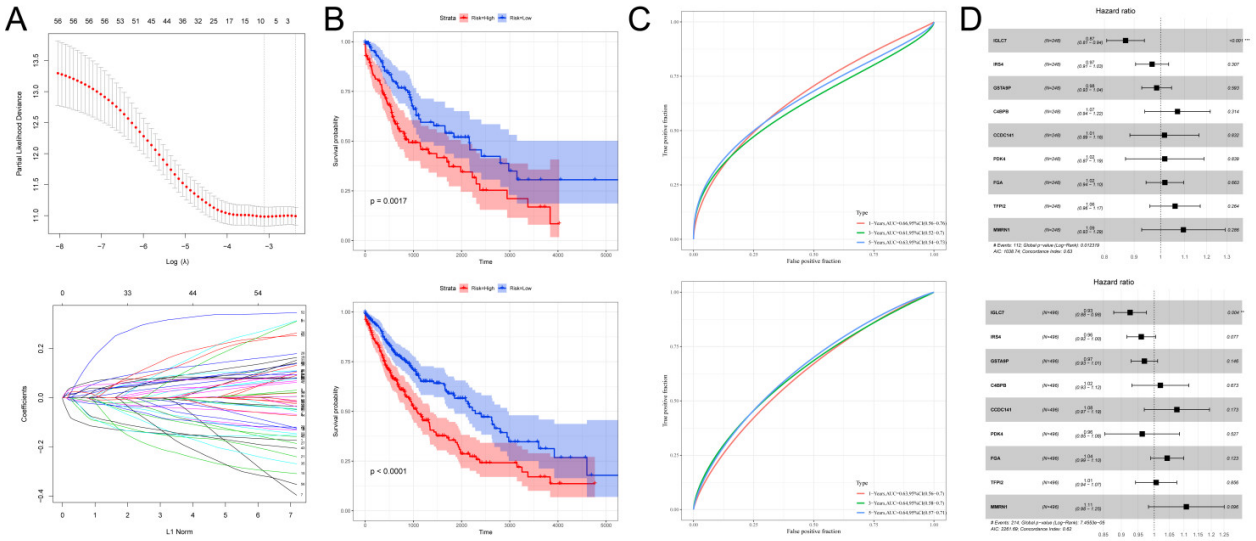

Figure 5. Survival modeling based on survival-related immune genes. (A) Lasso regression in the training set to determine the optimal genes. (B) Kaplan-Meier curves on risk scores in the training set and the overall dataset. (C) ROC analysis of the prognostic model, showing the AUC values of the prognostic model at 1 year, 3 years, and 5 years for the training set and the overall data set, respectively.

To further explore the impact of this survival model on the prognosis of LUSC patients, we created scatter plots of gene expression and corresponding survival times in different samples. The death rate gradually increased as the risk score increased, indicating that the survival model could predict the survival of LUSC patients (Figure 6A). As shown in Figure 6, risk score was significantly associated with survival in LUSC in the univariate COX regression model [hazard ratio (HR) = 2.1, 95% confidence interval (CI) = 1.6-2.9, p < 0.001]. In addition, multivariate Cox regression showed that risk score remained an independent predictor of prognosis in LUSC after adjusting for gender, T, M, and N stage (HR = 2.22, 95% CI = 1.68-2.9, p < 0.001). In addition, multivariate Cox regression showed that IGLC7, also known as immunoglobulin lambda constant 7, was an independent predictor of prognosis in LUSC after adjusting for individual gene expression profiles (HR = 0.87, 95% CI = 0.81-0.94, p < 0.001) (Figure 6B,C).

Based on the C-index values, a nomogram integrating the risk score, gender, and TNM stage was constructed. Total points were calculated by adding the points of the risk score, age, and TNM stage. The calibration curves for predicting 3- and 5-year OS (Overall Survival) showed that the survival rates predicted by the nomograms closely correlated with the actual survival outcomes (Figure 6D,E).

In addition, our analysis showed that the gene IGLC7 had the most significant effect on patient prognosis in this model. There are multiple pathways by which genes can influence patient prognosis, and immune-related genetic prognostic biomarkers are a potentially effective prognostic classifier. The effects of IGLC7 on immune cells and the synergistic effects of IGLC7 with other immune modulators are still largely unknown. To fill this gap, we explored the relevance of IGLC7 to immune cell populations, the synergistic effects of IGLC7 with immune checkpoints, and the relevance of IGLC7 to specific cellular immune and inflammatory responses.

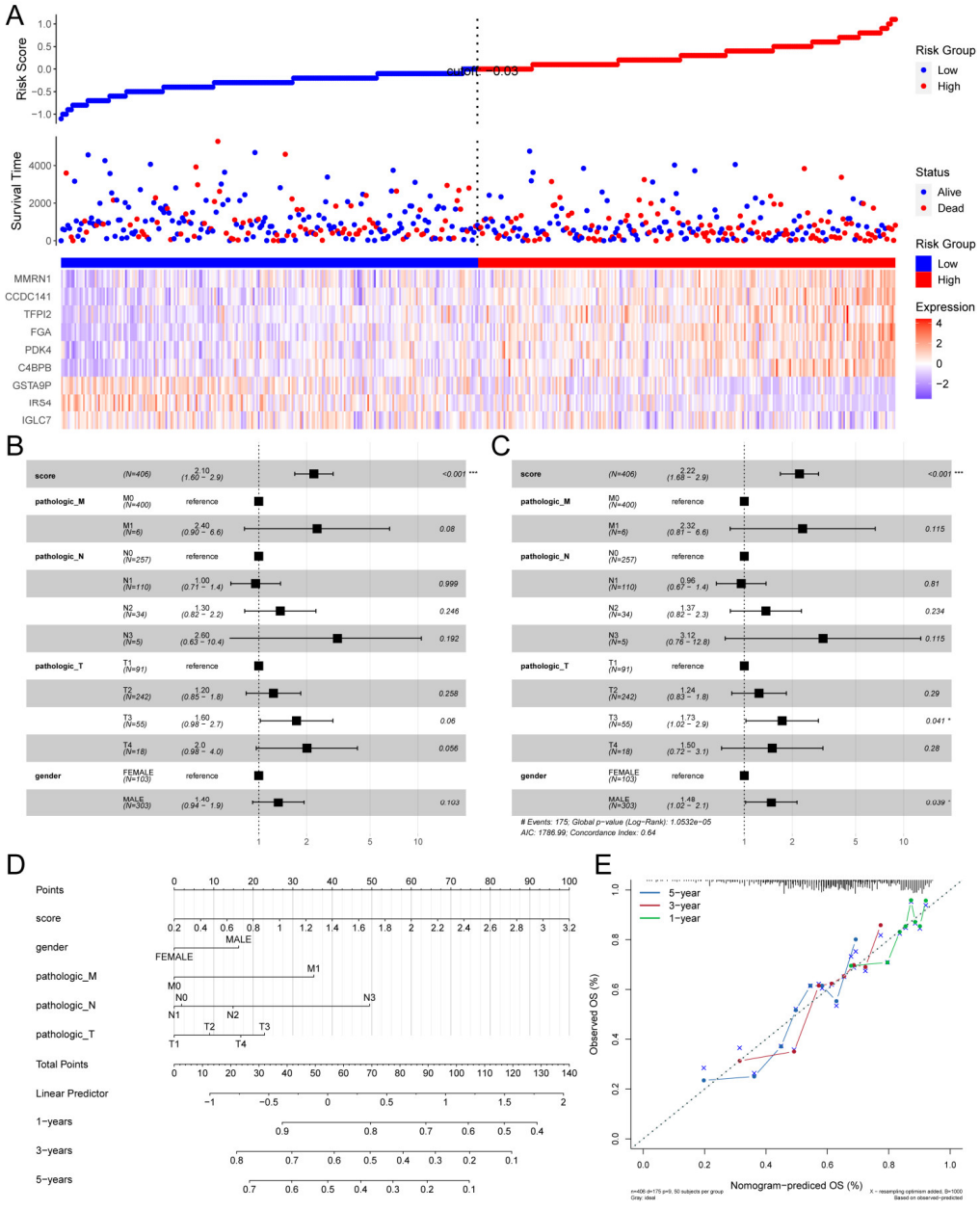

Figure 6. Prognostic values of the risk scores in The Cancer Genome Atlas LUSC. (A) Distribution of risk scores, along with survival statuses, and gene expression profiles for LUSC. (B, C) Univariate (B) and multivariate (C) Cox regression analyses of the risk score in LUSC regarding overall survival. (D) A nomogram for predicting 1-, 3- and 5-year survival possibilities of individual LUSC patients.

3.5. Relationship between IGLC7 expression and immune cell populations

In previous studies, only the physical location of human immunoglobulin lambda-like (IGLL) was demonstrated to be located on this gene, and its corresponding functional description is still unclear [12]. In patients with LUSC, the MCP-counter algorithm was used to calculate the absolute abundance of immune cell populations to clarify the immune manipulation function of IGLC7 further. Thus, as the expression of the IGLC7 gene increases, the expression abundance of immune cell populations likewise increases, indicating that IGLC7 expression plays a role in the immune response. Subsequently, we further calculated the correlation between IGLC7 and different immune cell populations. The marker genes for 24 immune cell species were used to predictthe abundance patterns of these cell populations in LUSC (Figure 7A). IGLC7 expression was strongly correlated with the immune cell population fractions of B cells (cor.p = 0.69), T cells (cor.p = 0.53), cytotoxic cells (cor.p = 0.48), regulatory T-cells (cor.p = 0.46), macrophages (cor.p = 0.44), T helper type 1cells (cor.p = 0.45) and T follicular helper cells (cor.p = 0.46), but less correlated with T helper 17cells, plasmacytoid dendritic cells, gamma delta T cells, and central memory T cells (Figure 7B). These results show that IGLC7 functions in T-cell and B-cell immune processes and is also involved in other cellular immune processes. This suggests that IGLC7 may possess multiple regulatory modes. Interestingly, other investigators have not revealed this result and may be a new insight for immunotherapy.

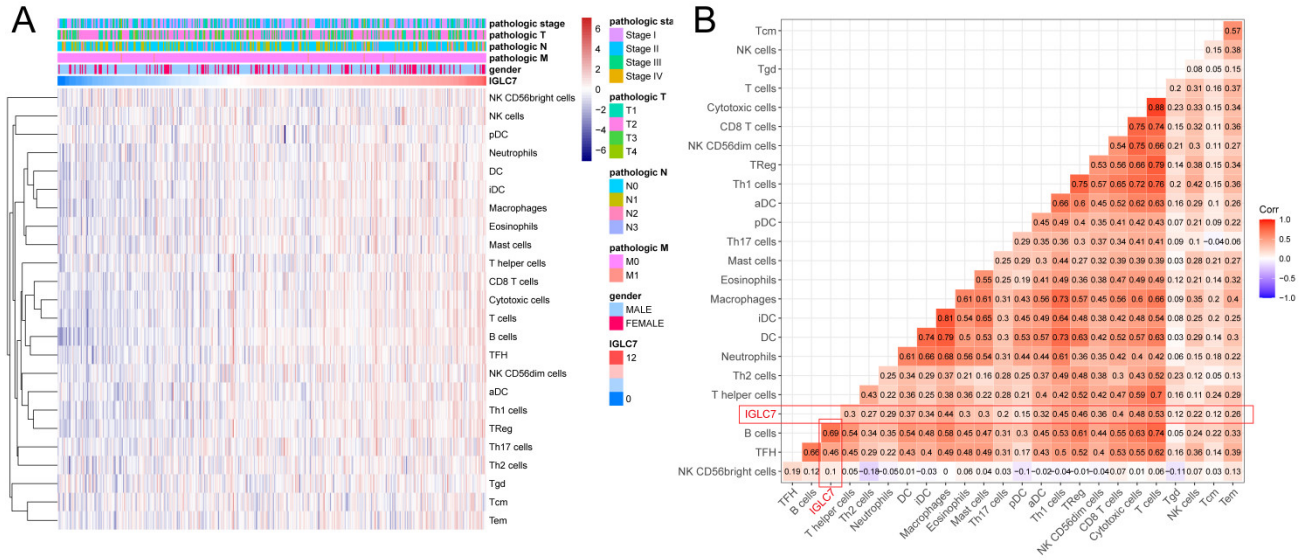

Figure 7. Relationship between IGLC7 expression and immune cell populations in the TCGA.

3.6. Association between IGLC7 expression and specific cell immune responses

In LUSC, the precise immunomodulatory function of IGLC7 is unclear. In order to investigate the immunomodulatory mechanisms of IGLC7, after analyzing the correlation between IGLC7 and immune cells, we performed a GSVA analysis of its correlation with specific immune pathways. Consistent with the above results, we found that IGLC7 was closely and positively associated with multiple immune pathways (Figure 8A), particularly the activation pathway of B cells and the positive regulatory pathway of T cell proliferation. This suggests a detailed immunological function of IGCL7

and not just a physical location overlap. This result indicates the potential of IGLC7 in regulating the immune response and could be a target for future studies.

3.7. Relationship between IGLC7 and inflammation

Table 3. 7 immune-related metagene sets.

HCK	IgG	Interferon	LCK	MHC_I	MHC_II	STAT1
C1QB	IGSF8	IFIT1	CD2	HLA-E	HLA-DRB1	TAP1
C1QA	ISLR2	IFIT3	GZMK	HLA-H	HLA-DRB5	STAT1
AIF1	IGSF21	IFI44L	GZMA	HLA-B	HLA-DRB3	CXCL10
LST1	IGSF1	OAS3	CD3D	HLA-J	HLA-DPA1	CXCL11
DOCK2	IGSF22	MX1	CD53	HLA-F	HLA-DRA	GBP1
LAPTM5	IGDCC3	RSAD2	LCK	HLA-G	HLA-DQA1	CXCL9
TYROBP	IGHD	IFI44	ARHGAP15	HLA-A	HLA-DQA2	
MS4A4A	IGSF11	OAS2	CCL5	HLA-C	HLA-DMA	
MS4A6A	IGSF5	OAS1	GMFG	HLA-L	HLA-DOA	
CD163	IGSF6		SELL		HLA-DRB4	
ITGB2			STAT4		HLA-DMB	
SLC7A7			SAMSN1		HLA-DQB1	
LAIR1			RAC2		HLA-DPB1	
HCK			HCLS1		HLA-DQB2	
TFEC			CCR7		CD74	
IFI30			PIK3CD		PTPRC	
MNDA			CORO1A		HLA-DOB	
FCER1G			CD48		HLA-DPB2	
RNASE6			IL2RG			
SLCO2B1			SH2D1A			
CCR1			SLAMF1			
			IL7R			
			INPP5D			
			KLRK1			
			FGL2			
			IRF8			
			SELPLG			
			IL10RA			
			SLA			
			CCR2			
			CSF2RB			

To provide further insight into the mechanisms by which IGLC7 mediates inflammatory activity, we used the GSVA algorithm to derive 104 genes from 7 clusters and defined them as metagenes associated with different inflammation and immune functions [13] (Table 3). These metagenes distinguished the prognosis of tumors in previous studies, and with this analysis, we identified a correlation between IGLC7 and the inflammatory response [14]. IGLC7 showed some degree of

positive correlation with the STAT1, LCK, HCK, MHC-I, MHC-II, IgG, and interferon gene clusters (Figure 8B). Among these seven clusters, IGLC7 showed the strongest correlation with LCK. Previous studies have shown LCK to be an important mediator of B-cell receptor signaling in other diseases [15], in addition to studies demonstrating that LCK can act as a novel prognostic-related gene [16]. Thus, IGLC7 might regulate various immune cells, which will help in improving the effectiveness of immunotherapy for LUSC.

3.8. Synergy of IGLC7 with other immune checkpoint members

We next evaluated the association of IGLC7 with other immune checkpoint members to further explore the synergistic role of IGLC7 in LUSC-induced immune responses, inflammatory pathways related to LUSC collected by Liu et al. [12,14] (Figure 8C). Detailed R and P values for the correlations between IGLC7 and other checkpoint members are listed in Table 4. We found that IGLC7 was closely associated with several checkpoint members, including CTLA4, BTLA, CD27, and CD48. Additionally, IGLC7 showed a positive correlation with all checkpoint members involved in the experiment, consistent with the correlation trend between IGLC7 and immune and inflammatory responses.

Table 4. Results of IGLC7 correlation with other immune checkpoints.

		cor	p
IGLC7	PDCD1LG2	0.3662468	0.00E+00
IGLC7	CD274	0.2390012	7.14E-08
IGLC7	CTLA4	0.4834565	0.00E+00
IGLC7	IDO1	0.3253724	1.07E-13
IGLC7	LAG3	0.3928751	0.00E+00
IGLC7	BTLA	0.5724124	0.00E+00
IGLC7	ICOS	0.4996488	0.00E+00
IGLC7	CD27	0.7278252	0.00E+00
IGLC7	CD40	0.1749747	8.95E-05
IGLC7	CD48	0.5439673	0.00E+00

Table 5. Inflammatory pathway annotation information.

ID	Description
GO:0050870:	positive regulation of T cell activation.
GO:0030217:	T cell differentiation;
GO:0042098:	T cell proliferation;
GO:0042102:	positive regulation of T cell proliferation;
GO:0042113:	B cell activation;
GO:0042129:	regulation of T cell proliferation;
GO:0050852:	T cell receptor signaling pathway;

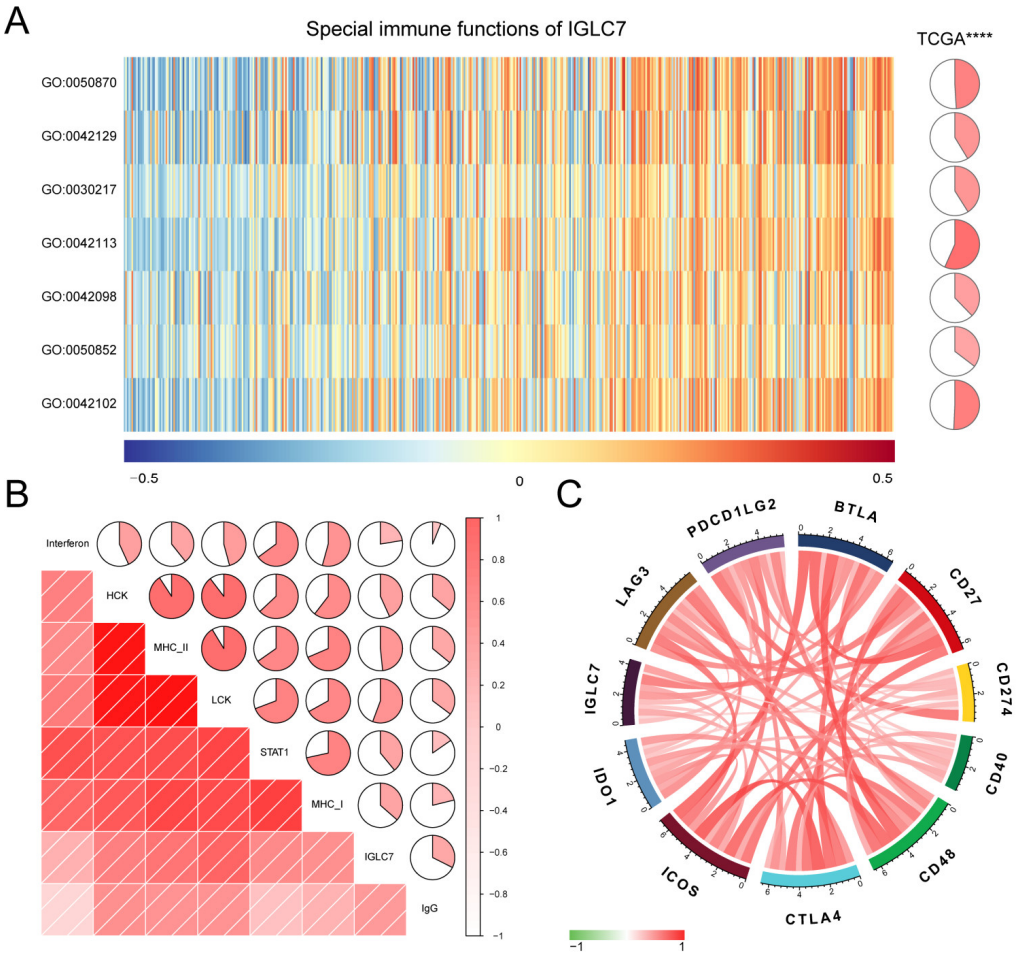

Figure 8. For IGLC7 systemic immunoassay (A) IGLC7-related cell immunity and inflammatory activities. (B) The relationship between IGLC7 and inflammatory activities. The pathway information is in Table 5. The pie denotes the correlation coefficient of IGLC7 and GO term. (C) IGLC7 expression is correlated with immune checkpoint members.

4. Discussion

In this study, we developed a survival model that can accurately predict the survival of LUSC patients through TCGA database mining and experimental validation. We identified IGLC7 as having the most significant effect on overall survival in LUSC patients, potentially becoming a new tumor microenvironment regulator. We assessed the correlation of IGLC7 with immune cell populations, synergy with other immune checkpoints, and correlation with specific cellular immune and inflammatory responses.

First, we generated scores for 496 LUSC patients, calculated the score distribution based on clinical information, and divided the patients into high and low immune score groups according to their immune scores. We found a significant difference between the high and low immune score groups in the Kaplan-Meier curves between the high and low score groups ($p = 0.039$). According to the survival differences between the different groups, we demonstrated that the level of immunity, as implied by the immune scores that had an impact on patient prognosis. By analyzing differential gene expression between the groups, we identified 1164 genes associated with immune infiltration in LUSC.

The 1164 DEGs obtained were subjected to GO and KEGG pathway analysis as well as GSEA analysis. Most of the genes, such as MS4A1, ADH7, and GPX2, were involved in regulating the tumor microenvironment [17,18]. GO terminology consistently showed that these DEGs interact with immune cells in the immune microenvironment of lung squamous carcinoma, with enriched terms including lymphocyte-mediated immunity, immune response-activating cell surface receptor signaling pathway, and adaptive immune response based on somatic recombination of immune receptors built from immunoglobulin superfamily domains. Similarly, KEGG pathway analysis also suggests that the genes are related to an immune response, with pathways involving autoimmune thyroid disease and intestinal immune network for IgA production being enriched. Consistent with GO and KEGG analysis, GSEA analysis also showed that this gene set is involved in regulating immune processes.

Then, using batch overall survival analysis, we performed an intersection set analysis and identified a total of 57 survival gene markers (Table 1). The GO and KEGG analysis results confirmed that the 57 genes associated with the prognosis of the patients were largely involved in immunomodulatory functions.

Of the 57 genes, we identified a novel survival-related immunomodulator, IGLC7, with independent predictive power based on our constructed model. The immune microenvironment has been shown to play an important role in the field of tumour biology and numerous therapeutic approaches, including immune checkpoint inhibitors, immunotherapy and gene therapy, play a powerful role in the treatment of cancer. Given the critical role of immune-related gene prognostic biomarkers in disease diagnosis and immunotherapy, we performed a multifaceted immune function analysis of IGLC7. To further elucidate the immune function of IGLC7 in LUSC, the abundance of immune cell populations was calculated using a microenvironmental cell population counting algorithm. The results indicate that IGLC7 is potentially associated with various immunomodulators and immune cells, demonstrating that IGLC7 may be involved in complex immune regulation and can become a new immunomodulator.

The immune activation of both T cells and B cells is considered to evaluate immune-related functions [16,17]. We found that IGLC7 is closely associated with T cell immunity and B cell immunity, implying a significant role in immune regulation. It was noted in previous studies that Memory $CD8^+$ T cells are critical in the immune process, but the development of vaccines targeting T cells remains problematic, mainly due to the limited knowledge of $CD8^+$ T cells. In our study, we found a high correlation between IGLC7 and T cells, and by targeting IGLC7 treatment may fill the current gap and provide a new idea. There is still a need for more in-depth studies on how other immune cells are involved in the immune process of tumors [18], but IGLC7 is shown here to act on the regulation of other immune cells. This implies a multimodal regulatory role for IGLC7 in LUSC and that IGLC7 plays an important immune and inflammatory regulatory function in LUSC.

5. Conclusions

In conclusion, IGLC7 expression levels are related to the malignancy of LUSC based on the constructed prognostic model and can thus be a therapeutic target for patients with LUSC. Furthermore, IGLC7 may work in concert with other immune checkpoint members to regulate the immune microenvironment of LUSC. These discoveries might lead to a fresh understanding of the complicated interactions between cancer cells and the tumor microenvironment, particularly the population of immune cells, and a novel approach to future immunotherapeutic treatments for patients with LUSC.

Acknowledgments

We would like to thank you for Jiangsu University medical clinical science technology development fund (JLY2021061) to support our work.

Conflict of interest

The authors declare there is no conflict of interest.

References

1. L. Gao, Y. N. Guo, J. H. Zeng, F. C. Ma, J. Luo, H. W. Zhu, et al., The expression, significance and function of cancer susceptibility candidate 9 in lung squamous cell carcinoma: A bioinformatics and in vitro investigation, *Int. J. Oncol.*, **54** (2019), 1651–1664. doi: 10.3892/ijo.2019.4758.
2. J. Xu, Y. Shu, T. Xu, W. Zhu, T. Qiu, J. Li, et al., Microarray expression profiling and bioinformatics analysis of circular RNA expression in lung squamous cell carcinoma, *Am. J. Transl. Res.*, **10** (2018), 771–783. Available from: https://www.ncbi.nlm.nih.gov/pmc/articles/PMC5883118/.
3. H. Lemjabbar-Alaoui, O. U. Hassan, Y. W. Yang, P. Buchanan, Lung cancer: Biology and treatment options, *Biochim. Biophys. Acta*, **1856** (2015), 189–210. doi: 10.1016/j.bbcan.2015.08.002.
4. C. A. Granville, P. A. Dennis, An overview of lung cancer genomics and proteomics, *Am. J. Respir. Cell Mol. Biol.*, **32** (2005), 169–76. doi: 10.1165/rcmb.F290.
5. D. Morgensztern, S. Waqar, J. Subramanian, F. Gao, R. Govindan, Improving survival for stage IV non-small cell lung cancer: A surveillance, epidemiology, and end results survey from 1990 to 2005, *J. Thorac. Oncol.*, **4** (2009), 1524–1529. doi: 10.1097/JTO.0b013e3181ba3634.
6. K. A. Gold, W. Ii, E. S. Kim, New strategies in squamous cell carcinoma of the lung: Identification of tumor drivers to personalize therapy, *Clin. Cancer Res.*, **18** (2012), 3002–3007. doi: 10.1158/1078-0432.CCR-11-2055.
7. Y. Kim, C. H. Kim, H. Y. Lee, S. H. Lee, H. S. Kim, S. Lee, et al., Comprehensive clinical and genetic characterization of hyperprogression based on volumetry in advanced non-small cell lung cancer treated with immune checkpoint inhibitor, *J. Thorac. Oncol.*, **14** (2019), 1608–1618. doi: 10.1016/j.jtho.2019.05.033.
8. B. Jing, T. Wang, B. Sun, J. Xu, D. Xu, Y. Liao, et al., IL6/STAT3 signaling orchestrates premetastatic niche formation and immunosuppressive traits in lung, *Cancer Res.*, **80** (2020), 784–797. doi: 10.1158/0008-5472.CAN-19-2013.
9. D. Hanahan, R. A. Weinberg, Hallmarks of cancer: the next generation, *Cell*, **144** (2011), 646–674. doi: 10.1016/j.cell.2011.02.013.
10. G. Bindea, B. Mlecnik, M. Tosolini, A. Kirilovsky, M. Waldner, A. C. Obenauf, et al., Spatiotemporal dynamics of intratumoral immune cells reveal the immune landscape in human cancer, *Immunity*, **39** (2013), 782–795. doi: 10.1016/j.immuni.2013.10.003.

11. R. C. Gentleman, V. J. Carey, D. M. Bates, B. Bolstad, M. Dettling, S. Dudoit, et al., Bioconductor: open software development for computational biology and bioinformatics, *Genome Biol.*, **5** (2004), R80. doi: 10.1186/gb-2004-5-10-r80.
12. T. R. Bauer, H. E. Mcdermid, M. L. Budarf, M. L. Van Keuren, B. B. Blomberg, Physical location of the human immunoglobulin lambda-like genes, 14.1, 16.1, and 16.2, *Immunogenetics*, **38** (1993), 387–399. doi: 10.1007/BF00184519.
13. A. Rody, U. Holtrich, L. Pusztai, C. Liedtke, R. Gaetje, E. Ruckhaeberle, et al., T-cell metagene predicts a favorable prognosis in estrogen receptor-negative and HER2-positive breast cancers, *Breast Cancer Res.*, **11** (2009), R15. doi: 10.1186/bcr2234.
14. Q. Liu, R. Cheng, X. Kong, Z. Wang, Y. Fang, J. Wang, Molecular and clinical characterization of PD-1 in breast cancer using large-scale transcriptome data, *Front. Immunol.*, **11** (2020), 558757. doi: 10.3389/fimmu.2020.558757.
15. F. Talab, J. C. Allen, V. Thompson, K. Lin, J. R. Slupsky, LCK is an important mediator of B-cell receptor signaling in chronic lymphocytic leukemia cells, *Mol. Cancer Res.*, **11** (2013), 541–554. doi: 10.1158/1541-7786.MCR-12-0415-t.
16. U. Rother, A. Grussler, C. Griesbach, V. Almasi-Sperling, W. Lang, A. Meyer, Safety of medical compression stockings in patients with diabetes mellitus or peripheral arterial disease, *BMJ Open Diabetes Res. Care*, **8** (2020). doi: 10.1136/bmjdrc-2020-001316.
17. T. W. Mudd, C. Lu, J. D. Klement, K. Liu, MS4A1 expression and function in T cells in the colorectal cancer tumor microenvironment, *Cell Immunol.*, **360** (2021), 104260. doi: 10.1016/j.cellimm.2020.104260.
18. R. Brigelius-Flohé, P. A. Kipp, Physiological functions of GPx2 and its role in inflammation-triggered carcinogenesis, *Ann. N. Y. Acad. Sci.*, **1259** (2012), 19–25. doi: 10.1111/j.1749-6632.2012.06574.x.

AIMS Press